

Evidence for a mixed CoNiO layer at the Co/NiO(001) interface from surface x-ray diffraction

C. Tusche,* H. L. Meyerheim, F. U. Hillebrecht,[†] and J. Kirschner*Max-Planck-Institut für Mikrostrukturphysik, Weinberg 2, D-06120 Halle, Germany*

(Received 11 November 2005; revised manuscript received 19 January 2006; published 3 March 2006)

The clean and cobalt-covered NiO(001) surface was studied by surface x-ray diffraction. The NiO(001) surface prepared by annealing in air at 1000 °C is characterized by a strong expansion of the top interlayer spacing ($\approx 14\%$ relative to the bulk NiO-spacing of 2.085 Å) and an outward relaxation (0.28 Å) of the oxygen atoms, which can be related to a high (27%) concentration of oxygen vacancy defects. In addition we find an oxygen-layer (most likely as part of the OH⁻ anion) on top of the surface Ni atoms at a distance of 2.33 Å. Deposition of 0.8 monolayers of Co induces a complex surface restructuring involving the formation of double layer CoO-islands above an oxygen deficient interfacial oxide layer ([NiCo]O_{0.5}) in registry with the underlying NiO single crystal. Our results support previous spectroscopic studies suggesting the presence of uncompensated interfacial spins responsible for the exchange bias.

DOI: [10.1103/PhysRevB.73.125401](https://doi.org/10.1103/PhysRevB.73.125401)

PACS number(s): 68.35.Ct, 68.47.Gh, 61.10.-i, 75.50.Ee

I. INTRODUCTION

Ultrathin ferromagnetic (FM) films grown on antiferromagnetic (AFM) oxides are of interest for fundamental studies of exchange biased systems. Although the effect of exchange bias was first discovered in 1956,¹ technological importance evolved not until the discovery of the giant magnetoresistance effect^{2,3} in 1988 followed by applications in hard-drive read heads and MRAM devices.⁴ In general, these devices involve complex structures where one of the FM layers is pinned by contact with an antiferromagnet. Exchange anisotropy at the FM/AFM interfaces gives rise to numerous effects like unidirectional or uniaxial anisotropies, which manifest in biased (shifted) magnetization loops or enhanced coercivity.⁵ In order to develop a comprehensive understanding of the FM/AFM junctions,^{6,7} a detailed knowledge of the buried FM/AFM interface is a prerequisite.

In general, the growth mode of an adlayer on a substrate is governed by the free surface energies of the respective species. Since in general the surface energy of oxides is lower than that of transition metals (TM's) three-dimensional island growth rather than layer by layer growth is expected for TM adsorption on TM oxides. The situation might become even more complex if interface reactions occur leading to an intermixed interface.

In this context, NiO represents a widely studied prototype system due to its high Néel-temperature (T_N) of 525 K and the simple rocksalt structure. A number of investigations have been carried out in the past, studying growth, interface chemistry, and magnetic properties of the TM/NiO adsorption systems.^{8–15}

X-ray photoemission spectroscopy (XPS), x-ray photoelectron diffraction (XPD), and low-energy electron diffraction⁸ (LEED) provided evidence for an intermixed interface and a partial reduction of NiO to Ni upon metal (Mn, Fe, Co) deposition. Improved surface ordering as evidenced from LEED after sample annealing at 700 K was attributed to the formation of CoO.

In qualitative agreement with this study, it was concluded from x-ray absorption (XAS) and x-ray circular dichroism

(XMCD) experiments^{9,11–13} that deposition of Co on NiO(001) leads to the formation of a CoNiO interface layer as a consequence of the reduction of NiO. Most importantly, the presence of metallic Ni was related to interfacial uncompensated spins suggested to be decisive for exchange bias and increased coercivity.¹³

On the basis of these studies a complex model of the Co/NiO(001) interface and its implications for modeling the mechanisms of exchange bias has evolved but no atomically resolved structure analysis has been carried out thus far. To this end we have studied the Co/NiO(001) interface using surface x-ray diffraction (SXR), which is a well established tool for analysis of surface structure and buried interfaces.¹⁶

II. EXPERIMENT

The experiments were carried out at the beamline ID03 of the European Synchrotron Radiation Facility using a six-circle ultrahigh-vacuum (UHV) diffractometer. Well established procedures for the preparation of NiO single crystal surfaces involve either cleaving under UHV conditions or repeated cycles of ion etching and annealing under oxygen atmosphere. While the first procedure is known to lead to a flat surface characterized by a low defect concentration, ion etching—although followed by annealing at 440 °C in oxygen atmosphere at $p_{O_2} \approx 10^{-6}$ mbar—was found to lead to an increasing surface roughness as determined by SXR spot profile measurements (see below).

For this reason a third approach was used: The crystal was heated to 1000 °C under ambient atmosphere for 12 h. After sample transfer into the UHV system no further preparation steps were applied and the quality of the crystal surface was checked by transverse scans¹⁷ over the (0 1 0.15) reflection, close to the (0 1 0) antiphase position.¹⁸ A full width at half maximum of 0.13° was determined, while for sputter annealed samples values close to 1° were obtained. This indicates that considerable surface roughness is introduced by the sputter-annealing process. No further check of the surface cleanliness was carried out at this point, since energetic electrons as used in Auger-electron spectroscopy (AES)

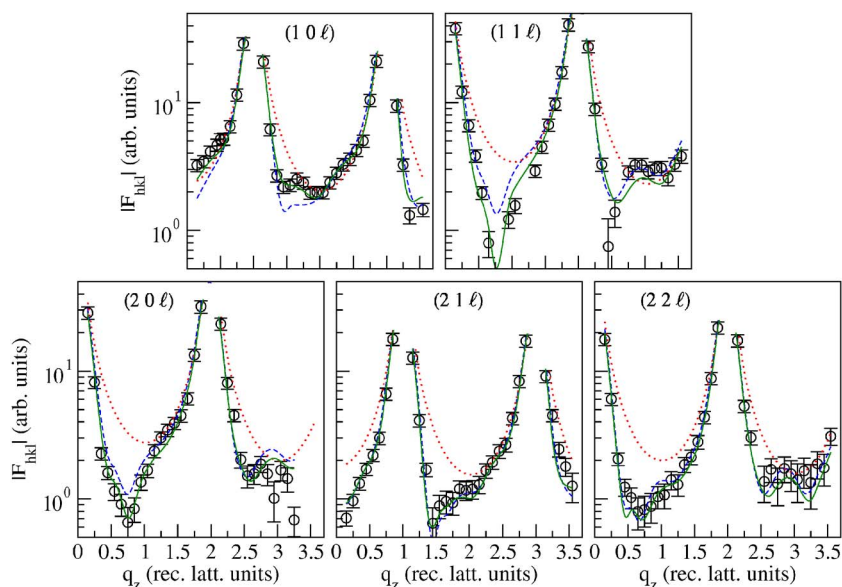


FIG. 1. (Color online) Experimental (circles) and calculated (lines) structure factor amplitudes along the $(1\ 0\ l)$, $(1\ 1\ l)$, $(2\ 0\ l)$, $(2\ 1\ l)$, and $(2\ 2\ l)$ CTR's for NiO(001). Solid lines represent the best fit characterized by oxygen vacancies, expansion of the first NiO interlayer spacing and an oxygen termination as shown in Fig. 3(a). Other structure models, neglecting the oxygen termination (dashed line) or simple bulk truncation (dotted line), lead to considerable deviations from the experimental data.

might affect the structure of the as-prepared sample which is characterized by an OH layer above the NiO(001) surface.

Cobalt was deposited on the NiO(001) surface kept at room temperature from a calibrated evaporator¹⁹ using a polycrystalline cobalt rod heated by electron beam bombardment. In total 0.8 monolayers (ML) were deposited, where we refer to one ML as 1 Co atom per (1×1) surface unit cell, i.e., 1.15×10^{15} atoms per cm^2 . AES spectra recorded at the end of the experimental run revealed the presence of some carbon, most likely due to CO contamination of the Co film deposited some hours before. It is thus concluded that the as-prepared bare NiO surface is not heavily contaminated by carbon.

Integrated x-ray reflection intensities were collected at grazing incidence of the incoming beam at a wavelength of 0.71 Å. In total, 153 (uncovered NiO) and 137 (Co/NiO) symmetry independent reflections were collected along the crystal truncation rods²⁰ (CTR's) $[(1\ 0), (1\ 1), (2\ 0), (2\ 1), \text{and } (2\ 2)]$ up to a maximum perpendicular momentum trans-

fer ($q_z = l \times c^*$) of 3.55 reciprocal lattice units (rlu, $1\ \text{rlu} = c^* = 0.661\ \text{Å}^{-1}$).

Open circles in Figs. 1 and 2 represent the experimental structure factor amplitudes $|F_{hkl}|$ along the crystal truncation rods (CTR's) for the as-prepared NiO(001) and Co-covered sample, respectively. While bulk reflections are characterized by integer coordinates (hkl) , crystal truncation leads to rods of intensity perpendicular to the surface. Therefore, the coordinate (l) of the momentum transfer normal to the surface becomes a continuous parameter, while the in-plane components retain their (1×1) surface periodicity with integer h and k .²⁰ Using the primitive setting of the surface unit cell¹⁸ ($a=b=2.94\ \text{Å}$, $c=4.17\ \text{Å}$), bulk Bragg reflections are characterized by the condition $h+k+l=2n$ (n integer).

The $|F_{hkl}|$'s were derived from the integrated intensities after correcting for instrumental factors.²¹ Standard deviations (σ) were estimated from the counting statistics and the reproducibility of symmetry equivalent reflections¹⁶ measured for the $(1\ 0)$, $(2\ 0)$, and $(2\ 1)$ CTR's. In Figs. 1 and 2

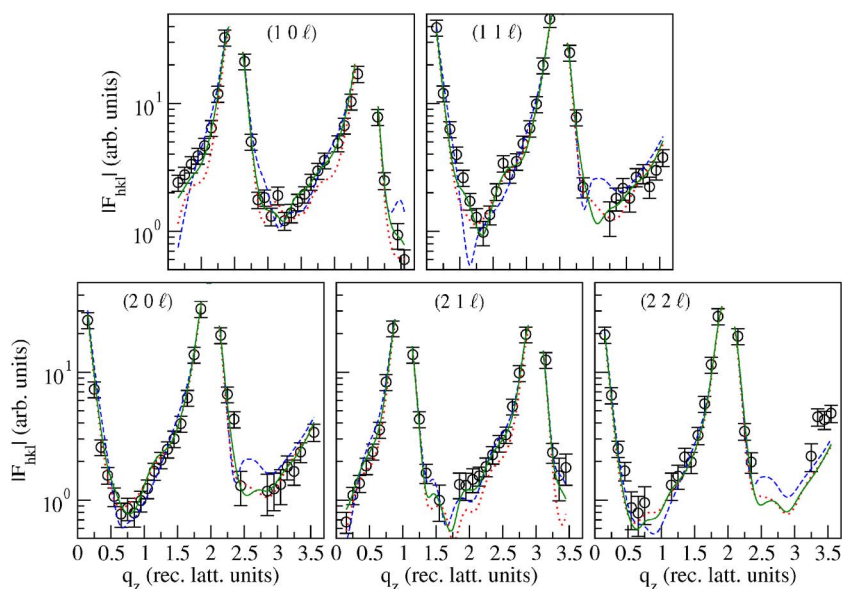


FIG. 2. (Color online) Experimental (circles) and calculated (lines) structure factor amplitudes on log-scale along the $(1\ 0\ l)$, $(1\ 1\ l)$, $(2\ 0\ l)$, $(2\ 1\ l)$, and $(2\ 2\ l)$ crystal truncation rods for 0.8 ML deposited on the as-prepared NiO(001) surface. The best fit (solid lines) represents a model with double-layer CoO islands on top of a mixed CoNiO layer with oxygen vacancies. Variations to this model with only one layer CoO (dashed lines) or a mixed CoNiO without vacancies (dotted line) are shown for comparison.

standard deviations are represented by the error bars. For all data sets σ is in the 10% range.

III. SXRD ANALYSIS OF NiO(001)

First, we discuss the structure of the as-prepared NiO(001) surface. Visual inspection of the experimental CTR's in Fig. 1 indicates a pronounced asymmetry of the intensity distribution relative to the antiphase condition. For comparison, the CTR's calculated for bulk truncated NiO(001) are characterized by symmetric U-shaped profiles as shown by the dotted lines in Fig. 1. Since the CTR minima are shifted to low q_z , an expansion of the top interlayer spacing is evident from the data without detailed analysis.

The quantitative structure analysis was carried out by least square fitting of the calculated structure factor amplitudes to the experimental ones. In total, four NiO-layers were included into the fit, including deeper layers did not lead to improvements. As a consequence of the high symmetry (plane group $p4mm$) of the body centered tetragonal structure¹⁸ there are only two independent positions per layer. The different species, Ni and O are located at $(0,0,z)$ and $(\frac{1}{2}, \frac{1}{2}, z)$ or vice versa, alternating layer by layer. Therefore, apart from an overall scale factor only two z parameters need to be refined per layer. In addition to the vertical positions also the isotropic Debye parameters (B) and fractional site occupancies were allowed to vary in order to simulate structural disorder, partial layer fillings, and non-stoichiometric phases. B is related to the mean square displacement of the atoms out of their equilibrium position $\langle u^2 \rangle$, by $B=8\pi^2\langle u^2 \rangle$.

A schematic structure model for NiO(001) including the interlayer spacings and the layer-resolved composition is shown in Fig. 3(a). The lengths of the bars represent the metal concentrations in fractions of a ML, only for the top O layer it indicates the oxygen occupancy. The layer stoichiometry is indicated by the labels inside the bars. Numbers on the right are the interlayer distances with reference to the Ni positions. They are given as differences relative to the bulk NiO interlayer spacing of 2.085 Å. Labels on the left indicate the vertical O positions relative to the plane of Ni atoms. In general, error bars are about 0.05 Å (2.4% of d_{bulk}) for the Ni and 0.1 Å for the O positions. In the following, several results can be summarized:

(i) For the spacing between the topmost NiO layers we determine an expansion of $\Delta d_{12} = +13.8\%$, while deeper layers do not show significant deviations from the bulk. There is a pronounced rumpling within the two topmost NiO layers, where the O atoms are located 0.28 Å above (first layer) and 0.09 Å below (second layer) the plane of the Ni atoms. As a consequence, the vertical Ni-O distances are considerably elongated up to the 2.6 Å range, which cannot be attributed to the distance between the ions in bulk NiO (2.085 Å).

(ii) On top of the surface Ni atoms an (incomplete) layer of oxygen atoms is found at a vertical distance of 2.33 Å. Whether or not this layer consists of oxygen ions only or these are part of an OH⁻ radical as suggested by McKay *et al.*²² cannot be identified by SXRD, since H atoms are “in-

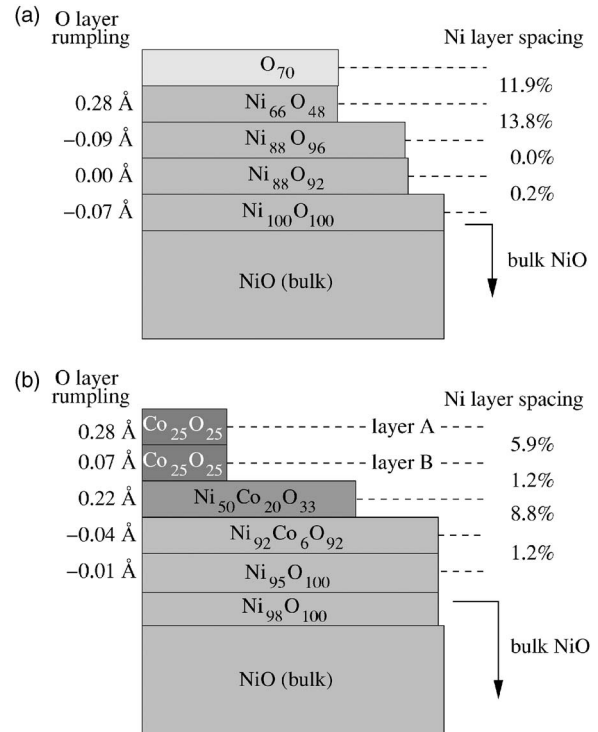


FIG. 3. Structure model for NiO(001) before (a) and after (b) cobalt deposition. Numbers on the right denote the interlayer spacings with reference to the metal atoms and are given as changes relative to the NiO bulk spacing. Numbers on the left indicate the vertical oxygen positions above (positive) or below (negative) the plane of the metal atoms.

visible” due to their low scattering amplitude. For this reason only O atoms are included in the fit.

(iii) Within the experimental uncertainty of about 10 percentage points for the determination of the occupancy factors, there is evidence that the top NiO layer is nonstoichiometric (Ni₆₆O₄₈), implying O-defect sites. Deeper NiO-layers are stoichiometric within the error bars, but seem not to be completely filled.

(iv) For the three topmost NiO layers we determine root-mean-square (r.m.s.) displacements ($\sqrt{\langle u^2 \rangle}$) in the range between 0.11 and 0.18 Å. For the OH-adsorbate layer we find 0.25 Å. Without temperature dependent measurements it is not possible to separate thermal disorder from the static one, but r.m.s. displacements in the 0.2–0.3-Å range as found for the OH adlayer at room temperature cannot be attributed to thermal vibrations only but must be attributed to static disorder.

On the basis of this model an excellent fit as shown by the solid lines in Fig. 1 is obtained. The CTR asymmetry induced by the large top layer expansion and all details—in particular the deep and sharp minima—are fitted very well. The considerable enhanced intensity variation along the rods as compared to the calculated rods for bulk truncated NiO(001) (dotted lines in Fig. 1) is related to surface roughness due to defects and the incompletely filled layers.

Quantitatively, the fit quality is measured by the goodness of fit (GOF) and the unweighted residuum (R_u).²³ We achieve GOF=1.4 and $R_u=0.10$. It should be emphasized

that the fit quality is very sensitive to structural details. For instance, the dashed lines represent the calculated CTR's neglecting the top oxygen layer. In this case—although the overall asymmetry of the CTR's is preserved—considerable deviations to the experimental data appear, which are most pronounced close to the minima. Correspondingly, the GOF equals to 2.1, which represents a 50% increase as compared to the best fit.

IV. SXRD ANALYSIS OF Co/NiO(001)

The CTR's derived for 0.8 ML Co deposited on the as-prepared NiO(001) surface are shown in Fig. 2. Comparison with those of the uncovered sample reveals a drop in intensity at the antiphase condition, while the asymmetry of the CTR's is preserved. The development of a meaningful structure model is complicated by the fact that Co is hardly distinguishable from Ni since the scattering lengths of both species are very similar. Therefore, the following assumptions were made, which are based on the knowledge of the NiO(001)-surface prior to cobalt deposition.

(i) Using the structure model for the as-prepared surface as a reference, the total amount of Ni in the surface region must remain constant upon Co deposition. Stated differently, deposited Co must be quantitatively reflected in the SXRD analysis by a correspondingly increased metal occupancy.

(ii) Similarly, the O concentration in the top NiO layers and the oxygen layer as determined for the uncovered sample represents an upper limit for the total amount of oxygen after Co deposition.

Taking into account these “boundary conditions” we could develop a model, which fits the experimental CTR's remarkably good. This is expressed by the GOF of 1.3 and an R_u of 0.14. In Fig. 2 the best fit is represented by the solid lines. The corresponding structure model is shown in Fig. 3(b). All labels have the same meaning as in Fig. 3(a).

In quantitative agreement with the calibrated amount of Co deposited (≈ 0.8 ML) the SXRD analysis yields an increase of the total amount of metal (Ni and Co) within the three uppermost layers. The SXRD analysis finds 0.76 ML of Co in excellent agreement with the calibration.

A considerable fraction (≈ 0.5 ML) of the deposited Co is oxidized and forms double layer CoO islands above of the topmost metal-oxide layer. Cobalt oxidation appears reasonable since sufficient oxygen is available on the as-prepared NiO surface. The remaining Co is found—albeit indirectly by an increase of the total metal concentration—in the first metal oxide layer. It should be noted that the question whether or not deeper layers contain an appreciable amount of Co is not directly accessible by the SXRD data. Since Co deposition was carried out with the sample kept at room temperature it is justified to assume that Co is concentrated mostly in the first layer, since excessive interdiffusion can be ruled out at this temperature.

In comparison with the as-prepared NiO(001) surface the most pronounced changes of the stoichiometry are observed in the first metal-oxide layer. While the O concentration is reduced from 48 to 33% of a ML, the total metal (Co+Ni) concentration is increased from 66 to 70%. Taking into ac-

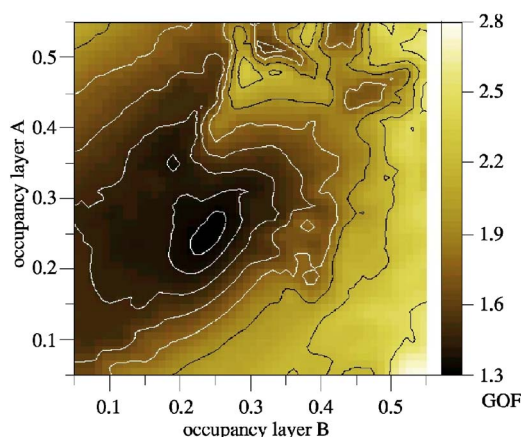


FIG. 4. (Color online) GOF versus CoO occupancy θ_A and θ_B in layers A and B [see Fig. 3(b)]. The scale is ranging from 2.8 (white) to 1.3 (black).

count that 50% of a ML of Co is incorporated within the oxide islands, an approximate Co concentration in the 20–30% range within the first layer is estimated. This leads to a mixed top metal-oxide layer, whose composition is $\text{Ni}_{150}\text{Co}_{20}\text{O}_{33}$ corresponding to a 2:1 metal excess as compared to a stoichiometric oxide. Allowing for this deviation from stoichiometry is a prerequisite for achieving a good fit. For comparison, the dotted lines in Fig. 2 represent the calculated CTR's for the 1:1 stoichiometric metal-oxide layer. At several places deviations are observed corresponding to a 12% increased GOF of 1.5.

It is also notable to see that the deeper layers are also affected although the changes relative to the as-prepared surface are almost within the error bars. We have evidence for some “filling” up of the NiO layers indicated by the increased fractional occupancy factors. In total, for the best fit we find 3.35 ML Ni within the top four NiO layers, while for the model of the as-prepared NiO(001) surface 3.42 ML were found. This is well within the experimental accuracy and is in agreement with condition (i) used for the model development as outlined above. The disorder within the NiO layers is the same as found for the as-prepared surface ($\sqrt{\langle u^2 \rangle} = 0.11\text{--}0.16$ Å). For the CoO layers we determine slightly larger values between 0.20 and 0.26 Å.

We have also studied the fractional occupancy of the CoO layers above the metal oxide. The total occupancy (θ) in the two CoO layers labeled by (A) and (B) in Fig. 3(b) is varied simultaneously preserving the CoO stoichiometry. All layer spacings throughout the structure were allowed to relax. Figure 4 shows the GOF versus θ_A and θ_B . Allowing only for structurally reasonable solutions characterized by $\theta_A \leq \theta_B$, the GOF minimum is in the region around $\theta_A \approx \theta_B = 25\%$. This gives evidence for a model with CoO double layer islands as expressed by the equal occupation in both layers. Within this model $\frac{1}{4}$ of the NiO surface is covered by CoO islands, while $\frac{3}{4}$ are left uncovered. The GOF minimum is quite broad corresponding to error bars of the order of $\Delta\theta = 10$ percentage points. Although this is a quite large uncertainty, it should be noted that the data nevertheless provide clear evidence for a CoO double layer. For instance, a model

characterized by 0.5 ML of CoO can be excluded, since it leads to a considerably worse fit as shown by the dashed lines in Fig. 2 and expressed by a GOF of 2.1.

V. DISCUSSION

The SXRD study of the as-prepared NiO(001) surface has revealed that an oxygen layer covers the topmost NiO layer, which is characterized by a $\text{Ni}_{66}\text{O}_{48}$ stoichiometry, i.e., there is a fraction of 27% of oxygen vacancies as compared to the ideal 1:1 NiO-stoichiometry.²⁴ Furthermore, there is evidence that deeper layers—although stoichiometric—are not completely filled. Adsorption of 0.8 ML of Co leads to a complex restructuring of the surface including an oxidation of about 0.5 ML of Co leading to a double layer of CoO islands above a mixed $\text{Ni}_{50}\text{Co}_{20}\text{O}_{33}$ layer. The detailed analysis of the interlayer spacings has revealed a significant expansion between the two topmost metal-oxide layers for both, the uncovered (13.8%) and the cobalt covered (8.8%) sample, implying enhanced vertical Ni-O distances up to the 2.6 Å range, i.e., considerably larger as compared to the distance between the ions in the bulk (2.086 Å).

Theoretical^{25–27} and experimental studies^{28–30} on flat NiO(001) as obtained for cleaved samples have revealed a 2–3 % contraction of the top layer spacing. For perfect ionic surfaces large relaxations are not expected.³¹ Therefore it is tempting to conclude that the expansion of the interlayer distances as derived for our sample can be attributed to surface structural defects. This conclusion is in good correspondence with previous studies on the NiO(001) surface, where surface defects were created using Ar^+ ion sputtering.

As pointed out by McKay *et al.*²² oxygen defects induce considerable modifications of the geometric and electronic structure. Since charge neutrality requires that two electrons must be trapped at the oxygen vacancy site, structural relaxations are expected as a consequence of the charge redistribution among the neighboring Ni sites. Simultaneously, ultraviolet photoemission spectroscopy (UPS) data clearly indicated the formation of a metallic surface state via a strong emission at the Fermi energy.

In a simple crystallochemical picture the increased Ni-O interatomic distance as found in the present study might be related to the defect induced charge redistribution leading to a reduced ionicity of the surface Ni atoms. The reduced ionicity is related to an increased radius and in turn to an enhanced interatomic distance. It should be emphasized that the determination of the top layer expansion is highly reliable and could even be anticipated by the pronounced asymmetry of the CTR's.

Furthermore, we observe a pronounced rumpling especially within the top NiO layer, where the oxygen atoms are located 0.28 Å above the plane of Ni atoms. Rumpling can also be related to the presence of surface defects,²² since for a defect free (001) surface recent calculations²⁷ do not suggest significant rumpling (there is one report, where even for a defect free surface a 0.2 Å outward oxygen displacement was predicted²⁵).

Oxygen vacancy defects, oxygen rumpling and the formation of an oxide (OH^-) layer are intimately related. The de-

fect free NiO(001) surface shows little interaction with gaseous molecular adsorbates,^{32,33} in particular no significant reactivity with O_2 or water is reported. In contrast, for the surface with oxygen defect sites, the situation is different. Interaction with O_2 and H_2O leads to the compensation of oxygen vacancies and the formation of a hydroxyl terminated surface is favored.^{22,32,34} Our experimental results also support the suggestion in Ref. 22 that top layer oxygen is located above the Ni plane. This is assumed to be induced by a reduced oxygen ionicity in the vacancy sites as compared to the O^{2-} ions in the bulk.

Our model for the Co/NiO(001) interface is also in well agreement with those derived on spectroscopic data.^{9,12,13} While cobalt adsorption leads to some smoothing of the surface region as determined on the basis of the layer resolved site occupancies for the second and third layer, it is interesting to see that the topmost CoNiO layer is characterized by an increased oxygen vacancy concentration²⁴ (54%) as compared to the as-prepared sample (27%). Although SXRD is not capable to provide direct information on the valence state of the different species, the increased deviation from the 1:1 stoichiometry can be interpreted by partial reduction of the top layer Ni-oxide phase upon cobalt deposition and the presence of a fraction of a ML of metallic Ni and Co. While in Ref. 12 no evidence was found for the formation of stoichiometric CoO, a double CoO layer is determined for our sample. Most likely this is because of the presence of the top oxide (OH^-) layer in the as-prepared sample. In contrast, the NiO surface in Ref. 12 was prepared by crystal cleavage or Ni evaporation in oxygen atmosphere, where this layer was not present.

The Co coverage determined by the SXRD analysis is in good correspondence with the expected Co coverage based on the calibration of the evaporator. It is therefore concluded that all or almost all of the deposited cobalt (≈ 0.8 ML) is in registry with the underlying bulk lattice, since only in this case there is a contribution of the cobalt atoms to the integer order CTR's.

Therefore the $\text{CoNiO}_{0.5}$ layer is in a structurally well ordered arrangement. This is a nontrivial and important result, since apart from its stoichiometry, also the lattice strain of the mixed $\text{CoNiO}_{0.5}$ layer might be decisive for its magnetic properties. In contrast to CoO, whose bulk lattice constant (4.25 Å) is well matched to NiO (4.19 Å), there is a misfit as large as 18% to the corresponding metals (Co_{fcc} : 3.54 Å, Ni_{fcc} : 3.52 Å).

Equilibrium lattice parameters for substoichiometric TM-oxide phases are not known, but considering the spectroscopic evidence suggesting the presence of a small amount of metal in the mixed layer, it must be concluded that it is in a highly strained state, when in registry with NiO. In this context, magnetoelastic contributions might then become important for the magnetic interface properties, since these are known to largely influence the anisotropy energy even in cases where strains are in the percent regime.³⁵

VI. SUMMARY

We have carried out a detailed x-ray structure analysis of NiO(001) prepared by annealing at 1000 °C in air and after

deposition of about 0.8 ML cobalt. For the bare NiO(001) surface the top NiO-layer is characterized by a large concentration of oxygen vacancy defects. Simultaneously, considerable structural relaxations such as a 14% enhanced top layer spacing and surface layer rumpling is observed. Above the top metal-oxide layer we determine an oxygen layer, which is attributed to OH⁻-ions resulting from H₂O adsorption on the defect surface.

Cobalt adsorption on the as-prepared sample leads to a complex restructuring of the surface characterized by a substoichiometric CoNiO_{0.5} interface with a metal:oxygen ratio of about 2:1. Above this layer double layer CoO-islands are formed due to the oxidation of arriving Co atoms by surface oxygen or hydroxyl ions.

Our structure analysis supports recent investigations using x-ray absorption spectroscopy and x-ray magnetic dichroism where reduction of nickel by cobalt is proposed leading to the formation of metallic Ni. The latter was found to give a ferromagnetic contribution, considered important for exchange bias.

ACKNOWLEDGMENTS

The authors would like to thank the ESRF for the hospitality during their stay. The help of C. Quiros during the experiments is also gratefully acknowledged.

*Electronic address: tusche@mpi-halle.mpg.de; URL: <http://www.mpi-halle.mpg.de>

†Present address: Institut für Festkörperforschung, Forschungszentrum Jülich, D-52425 Jülich, Germany.

¹W. H. Meiklejohn and C. P. Bean, *Phys. Rev.* **102**, 1413 (1956).

²M. N. Baibich, J. M. Broto, A. Fert, F. NguyenVanDau, F. Petroff, P. Eitenne, G. Creuzet, A. Friederich, and J. Chazelas, *Phys. Rev. Lett.* **61**, 2472 (1988).

³G. Binasch, P. Grünberg, F. Saurenbach, and W. Zinn, *Phys. Rev. B* **39**, 4828 (1989).

⁴G. A. Prinz, *Sci. Compass* **282**, 1660 (1998).

⁵J. Nogués and I. K. Schuller, *J. Magn. Magn. Mater.* **192**, 203 (1999).

⁶R. L. Stamps, *J. Phys. D* **33**, R247 (2000).

⁷Z. Qian and J. M. Sivertsen, *J. Appl. Phys.* **83**, 6825 (1998).

⁸R. de Masi, D. Reinicke, F. Müller, P. Steiner, and S. Hüfner, *Surf. Sci.* **515**, 523 (2002).

⁹T. J. Regan, H. Ohldag, C. Stamm, F. Nolting, J. Lüning, J. Stöhr, and R. L. White, *Phys. Rev. B* **64**, 214422 (2001).

¹⁰P. Luches, M. Liberati, and S. Valeri, *Surf. Sci.* **532-535**, 409 (2003).

¹¹H. Ohldag, A. Scholl, F. Nolting, S. Anders, F. U. Hillebrecht, and J. Stöhr, *Phys. Rev. Lett.* **86**, 2878 (2001).

¹²H. Ohldag, T. J. Regan, J. Stöhr, A. Scholl, F. Nolting, J. Lüning, C. Stamm, S. Anders, and R. L. White, *Phys. Rev. Lett.* **87**, 247201 (2001).

¹³H. Ohldag, A. Scholl, F. Nolting, E. Arenholz, S. Maat, A. T. Young, M. Carey, and J. Stöhr, *Phys. Rev. Lett.* **91**, 017203 (2003).

¹⁴C. Mocuta, A. Barbier, G. Renaud, and B. Dieny, *Thin Solid Films* **336**, 160 (1998).

¹⁵C. Mocuta, A. Barbier, G. Renaud, M. Panabièrre, and P. Bayle-Guillemaud, *J. Appl. Phys.* **95**, 2151 (2004).

¹⁶I. K. Robinson and D. J. Tweet, *Rep. Prog. Phys.* **55**, 599 (1992).

¹⁷R. Feidenhans'l, *Surf. Sci. Rep.* **10**, 105 (1989).

¹⁸We use a sample setting corresponding to a primitive surface unit cell, where the surface (*s*) setting is related to the face centered

cubic setting of the bulk (*b*) by the following relations: $[100]_s = 1/2 \times ([100]_b - [010]_b)$; $[010]_s = 1/2 \times ([100]_b + [010]_b)$ and $[001]_s = [001]_b$.

¹⁹J. Kirschner, H. Engelhard, and D. Hartung, *Rev. Sci. Instrum.* **73**, 3853 (2002), and references therein.

²⁰I. K. Robinson, *Phys. Rev. B* **33**, 3830 (1986).

²¹E. Vlieg, *J. Appl. Crystallogr.* **30**, 532 (1997).

²²J. M. McKay and V. E. Henrich, *Phys. Rev. B* **32**, 6764 (1985).

²³The goodness of fit is defined as $GOF = \sqrt{\chi^2} = \sqrt{\sum \sigma^{-2} (|F_{obs}| - |F_{calc}|)^2 / (N - P)}$ and R_u is defined as $R_u = \sum ||F_{obs}| - |F_{calc}|| / \sum |F_{obs}|$, where σ is the standard deviation, P the number of free parameters, and F_{obs} and F_{calc} are the observed and calculated structure factors, respectively; the summation runs over all N datapoints.

²⁴The concentration of oxygen vacancy sites is given relative to the occupied metal sites in this layer. 0% means the stoichiometric oxide.

²⁵H. Nakatsugawa and E. Iguchi, *Surf. Sci.* **357-358**, 96 (1996).

²⁶T. E. Karakasidis, D. G. Papageoriou, and G. A. Evangelakis, *Appl. Surf. Sci.* **162-163**, 233 (2000).

²⁷O. Begone, M. Alouani, J. Hugel, and P. Blöchl, *Comput. Mater. Sci.* **24**, 192 (2002).

²⁸C. G. Kinniburgh and J. A. Walker, *Surf. Sci.* **63**, 274 (1977).

²⁹M. R. Welton-Cook and M. Prutton, *J. Phys. C* **13**, 3993 (1980).

³⁰M. Prutton, J. A. Walker, M. R. Welton-Cook, and R. C. Felton, *Surf. Sci.* **89**, 95 (1979).

³¹D. Wolf, *Phys. Rev. Lett.* **68**, 3315 (1992).

³²D. Cippus, C. Xu, D. Ehrlich, B. Dillmann, C. A. Ventrice, Jr., K. Al Shamery, H. Kühlenbeck, and H. J. Freund, *Chem. Phys.* **177**, 533 (1993).

³³M. Schönnenbeck, D. Cippus, J. Klinkmann, H. J. Freund, L. G. M. Petterson, and P. S. Bagus, *Surf. Sci.* **347**, 337 (1995).

³⁴R. Kubiak, H. Morgner, and O. Rakhovskaya, *Surf. Sci.* **321**, 229 (1994).

³⁵D. Sander, *Rep. Prog. Phys.* **62**, 809 (1999).